The Astrophysical Journal, 838:148 (14pp), 2017 April 1 https://doi.org/10.3847/1538-4357/aa64d7

OmegaWINGS: The First Complete Census of Post-starburst Galaxies in Clusters in the Local Universe

A. Paccagnella[1,2], B. Vulcani[3], B. M. Poggianti[2], J. Fritz[4], G. Fasano[2], A. Moretti[2], Yara L. Jaffé[5], A. Biviano[6], M. Gullieuszik[2], D. Bettoni[2], A. Cava[7], W. Couch[8], and M. D'Onofrio[1,2]

[1] Department of Physics and Astronomy, University of Padova, Vicolo Osservatorio 3, I-35122 Padova, Italy
[2] INAF—Astronomical Observatory of Padova, I-35122 Padova, Italy
[3] School of Physics, University of Melbourne, VIC 3010, Australia
[4] Instituto de Radioastronomía y Astrofísica, IRyA, UNAM, Campus Morelia, A.P. 3-72, C.P. 58089, Mexico
[5] European Southern Observatory, Alonso de Cordova 3107, Vitacura, Casilla 19001, Santiago de Chile, Chile
[6] INAF—Astronomical Observatory of Trieste, I-34143 Trieste, Italy
[7] Observatoire de Genève, Universitè de Genève, 51 Ch. des Maillettes, 1290 Versoix, Switzerland
[8] Australian Astronomical Observatory, PO Box 915, North Ryde, NSW 1670, Australia
Received 2016 September 1; revised 2017 February 26; accepted 2017 March 1; published 2017 April 4

Abstract

Galaxies that abruptly interrupt their star formation in <1.5 Gyr present recognizable features in their spectra (no emission and Hδ in absorption) and are called post-starburst (PSB) galaxies. By studying their stellar population properties and their location within the clusters, we obtain valuable insights on the physical processes responsible for star formation quenching. We present the first complete characterization of PSB galaxies in clusters at $0.04 < z < 0.07$, based on WINGS and OmegaWINGS data, and contrast their properties to those of passive (PAS) and emission-line (EML) galaxies. For $V < 20$, PSBs represent $7.2 \pm 0.2\%$ of cluster galaxies within 1.2 virial radii. Their incidence slightly increases from the outskirts toward the cluster center and from the least toward the most luminous and massive clusters, defined in terms of X-ray luminosity and velocity dispersion. The phase-space analysis and velocity-dispersion profile suggest that PSBs represent a combination of galaxies with different accretion histories. Moreover, PSBs with the strongest Hδ are consistent with being recently accreted. PSBs have stellar masses, magnitudes, colors, and morphologies intermediate between PAS and EML galaxies, typical of a population in transition from being star-forming to passive. Comparing the fraction of PSBs to the fraction of galaxies in transition on longer timescales, we estimate that the short-timescale star formation quenching channel contributes two times more than the long timescale one to the growth of the passive population. Processes like ram-pressure stripping and galaxy–galaxy interactions are more efficient than strangulation in affecting star formation.

Key words: galaxies: clusters: general – galaxies: evolution – galaxies: formation – galaxies: star formation

1. Introduction

The galaxy population can be thought of as bimodal, with star-forming late-type galaxies populating the so-called blue cloud and passive early-type galaxies preferentially found in the red sequence (Blanton et al. 2003; Kauffmann et al. 2003, 2004; Baldry et al. 2004; Balogh et al. 2004; Brinchmann et al. 2004). This bimodality is strongly correlated with the environment, with many studies pointing out a well-established morphology–density relation holding in both clusters and the field: the higher the projected surface density of galaxies within an area, the higher is the fraction of early types and the lower is the fraction of late types (e.g., Dressler 1980; Dressler et al. 1997; Baldry et al. 2004; Fasano et al. 2015). This piece of evidence indicates a role of the environment in shaping galaxy properties.

The detection of a conspicuous population of star-forming galaxies in the core of rich and dense clusters at $z \sim 0.5$, but absent today (Butcher & Oemler 1984), was the first discovery of a strong decline in star formation with time. Subsequently, several studies (e.g., Poggianti et al. 1999; Cooper et al. 2008) have shown the influence of high-density environments on the formation and evolution of galaxies. In an evolutionary scenario in which clusters form and grow through the accretion of field galaxies, these findings suggest that there should be some active mechanisms able to halt the star formation in infalling galaxies. Several authors proposed many different mechanisms able to shut down star formation in high-density regions; examples include ram-pressure stripping (Gunn & Gott 1972), high-speed galaxy encounters (galaxy harassment; Moore et al. 1996), galaxy–galaxy mergers (Mihos & Hernquist 1994), and removal of the warm and hot halo gas (strangulation; Larson et al. 1980; Balogh et al. 2000). Recently, Dressler et al. (2013) proposed that cluster galaxies could be transformed via group pre-processing, during the fall-in group phase.

Valuable insights to understand how the star-forming population turns passive can be obtained by studying galaxies that appear to have intermediate properties and may be in the act of transitioning between the two main galaxy populations. This transition can occur on different timescales depending on the main process inducing the transformations (Mok et al. 2013; Wetzel et al. 2013; Schawinski et al. 2014; Wheeler et al. 2014; Vulcani et al. 2015; Paccagnella et al. 2016). However, a clear picture describing the reasons why galaxies turn passive following different paths and the properties of these galaxies is still lacking.

Dressler & Gunn (1982), investigating cluster galaxies at intermediate redshifts, found a large number of spectra showing strong Balmer absorption lines and no emission and called them post-starburst (PSB) galaxies. These features are typical of stellar populations in which star formation had ended abruptly within the last 1–1.5 Gyr and therefore should have been affected by some of the aforementioned processes.

Since then, extensive spectrophotometric modeling (Couch & Sharples 1987; Newberry et al. 1990; Abraham et al. 1996; Poggianti & Barbaro 1996, 1997; Bekki et al. 2001; Poggianti 2004) has found that the presence of strong hydrogen lines in absorption and the concomitant absence of emission lines, indicating no ongoing star formation, can be explained roughly decomposing the spectra into a combination of a K-giant-star (or early-type galaxy) spectrum and an A-star spectrum, Such decomposition is at the origin of the name "$k+a$," often used to describe PSB galaxies. In general, A-type stars—i.e., newborn stars formed within the last 1 Gyr whose spectra are characterized by strong Balmer absorption lines—dominate the light of a galaxy about 0.5 Gyr after star formation stopped and leave their signature on the spectra visible for 1–1.5 Gyr. In contrast, O and B stars—more massive stars that die very quickly and emit the energetic photons able to ionize the gas and produce emission lines—have no or very little contribution. This combination can appear as a result of a star-bursting episode observed shortly after the star formation has stopped (for those galaxies with the strongest Balmer lines), or as a consequence of normal star formation that has been abruptly ended. Moreover, since A-type stars have known lifetimes, the evolution of this population can be used as a quenching clock.

The reason why PSB galaxies underwent an episode of star formation that was abruptly stopped is still matter of debate; any of the mentioned quenching mechanisms acting on a short timescale could trigger a starburst and cease star formation, producing a $k+a$ spectra. Important hints for solving this matter come from the study of the galaxy environments as different quenching mechanisms play different roles in different environments.

Galaxy mergers could be the dominant mechanism in the field at low-z, where recent studies found a significant fraction of PSB galaxies (Bekki et al. 2001; Blake et al. 2004; Quintero et al. 2004; Goto 2005; Hogg et al. 2006; Mahajan 2013), but they are less effective in clusters, due to the high velocity dispersions.

The origin of $k+a$ galaxies in clusters is more probably related to the interaction of the infalling population with the hot and dense intracluster medium (ICM). Indeed, as suggested by Dressler & Gunn (1982), Couch & Sharples (1987), Dressler & Gunn (1992), Poggianti et al. (1999), Tran et al. (2003), Tran et al. (2004), Tran et al. (2007), and Poggianti et al. (2009), the interaction of a gas-rich galaxy with the hot high-pressure ICM via ram-pressure stripping might trigger a starburst and then clear the disk of neutral gas stopping star formation. The most striking evidence for this is perhaps in the Coma cluster, where the position of young PSB galaxies is strongly correlated with strong X-ray temperature gradients (Poggianti 2004). While this picture is corroborated by observations of high and intermediate redshift clusters (Poggianti et al. 1999; Muzzin et al. 2014), in the local universe, several works (e.g., Blake et al. 2004; Goto 2005) found that PSB galaxies prefer low-density environments and thus assess that cluster-specific processes are not likely to be the dominant source of fast quenching. Nonetheless, the few studies that investigated the fraction and properties of the local PSB cluster population (e.g., Caldwell & Rose 1997; Poggianti 2004; Fritz et al. 2014) found evidence of truncated star formation in a significant fraction of cluster members. A complete census of PSB galaxies in clusters and a homogeneous comparison with the field population is, however, still lacking. The main reasons are the paucity of the cluster samples studied and the different selection criteria adopted in these studies that do not allow fair intra-sample comparisons. In addition, local PSB galaxies are often selected without constraints on the Hα line, to allow for direct comparisons with high-redshift samples, where generally the spectral coverage does not allow to reach the Hα emission. However, as shown by Goto et al. (2003) and Blake et al. (2004), such selections suffer from high levels ($\approx$50%) of contamination from Hα emitting galaxies.

In this work, we exploit a sample of galaxies in clusters drawn from the WIde-field Nearby Galaxy-cluster Survey (WINGS; Fasano et al. 2006; Moretti et al. 2014) and OmegaWINGS surveys (Gullieuszik et al. 2015; Moretti et al. 2017). The combination of the two projects allows us to study the properties of $\sim$10,000 member galaxies in an homogeneous sample at $0.04 < z < 0.07$. This data set is unique, as none of the other low-z surveys investigate a large sample of clusters and cluster galaxies in such detail. Thanks to the wide area covered by OmegaWINGS ($\sim$1deg^2), we can investigate cluster members well beyond the cluster virial radius and link clusters with the surrounding population and the field that have been proved to be essential for understanding galaxy transformations (Lewis et al. 2002; Pimbblet et al. 2002; Treu et al. 2003; Moran et al. 2007; Marziani et al. 2016).

We investigate the occurrence and properties of PSB galaxies in 32 clusters and compare them to those of passive and star-forming galaxies. Trends are investigated as a function of both cluster-centric distance and global cluster properties, i.e., cluster velocity dispersion and X-ray luminosity. The aim of this analysis is to shed light on the processes acting on these galaxies and the timescale needed to transform from one type to the other.

The paper is organized as follows. Section 2 presents the data set and the main galaxy properties; Section 3 summarizes the spectroscopic classification; Section 4 presents the data sample. Section 5 presents our results, focusing on the analysis of the PSB galaxy population and comparing it to the complementary samples of star-forming and passive galaxies. Morphologies, spatial distributions, and dependencies on global cluster properties are inspected. Finally, we discuss our results in Section 6 and conclude in Section 7.

Throughout the paper, we adopt a Salpeter (1955) initial mass function in the mass range 0.15–120 $M_\odot$. The cosmological constants assumed are $\Omega_m = 0.3$, $\Omega_\Lambda = 0.7$, and $H_0 = 70\,\mathrm{km\,s^{-1}\,Mpc^{-1}}$.

2. Data Set and Galaxy Properties

We base our analysis on WINGS (Fasano et al. 2006; Moretti et al. 2014), a multi-wavelength survey of 76 clusters of galaxies with $0.04 < z < 0.07$ X-rays selected from *ROSAT* All Sky Survey data (Ebeling et al. 1996, 1998, 2000), and from its recent extension, OmegaWINGS, which includes new observations for 46 of these clusters (Gullieuszik et al. 2015; Moretti et al. 2017). The cluster samples cover a wide range of velocity dispersion ($\sigma_{\rm cl} \sim$ 500–1300 km s^{-1}) and X-ray luminosity ($L_X \sim 0.2$–5×10^{44} erg s^{-1}).

The WINGS survey is mainly based on optical B, V imaging (Varela et al. 2009) that covers a $34' \times 34'$ field of view, corresponding to at least about a cluster-centric distance of $0.6R_{200}$. R_{200} is defined to be the radius delimiting a sphere with an interior mean density 200 times the critical density and is

used as an approximation for the cluster virial radius. The survey has been complemented by a spectroscopic survey for a subsample of 48 clusters, obtained with the spectrographs WYFFOS@WHT and 2dF@AAT (Cava et al. 2009), by a near-infrared (J, K) survey for a subsample of 28 clusters obtained with WFCAM@UKIRT (Valentinuzzi et al. 2009), and by U broadband and Hα narrowband imaging for a subsample of 17 clusters, obtained with wide-field cameras at different telescopes (INT, LBT, Bok; Omizzolo et al. 2014).

OmegaWINGS extends the WINGS survey in terms of cluster spatial coverage: OmegaCAM/VST imaging in the u, B, and V bands have been obtained for 45 fields covering 46 WINGS clusters over an area of $\sim$1 deg^2 (Gullieuszik et al. 2015), thus allowing us to investigate trends well beyond the virial radius and connect clusters with the surrounding population and the field. The spectroscopic follow-up has been obtained for a subsample of 33 clusters with the 2dFdr@AAT (Moretti et al. 2017).

The target selection was similar for the two surveys (Cava et al. 2009; Moretti et al. 2017). It was based on the available optical B, V photometry (Varela et al. 2009; Gullieuszik et al. 2015) and aimed at maximizing the chances of observing galaxies at the cluster redshift without biasing the cluster sample. Targets were selected to have a total magnitude brighter than $V = 20$, excluding only those well above the color–magnitude sequence with $B - V > 1.20$. These criteria minimize the contamination from background galaxies and include all galaxies on and below the red sequence up to $z \sim 0.08$.

Combining the data of the two surveys, the final spectroscopic sample consists of 22674 spectra in 60 clusters (Moretti et al. 2017).

To measure spectroscopic redshifts, we adopted a semi-automatic method, which involves the automatic cross-correlation technique and emission line identification, with a very high success rate ($\approx$95% for the whole sample, see Cava et al. 2009 and Moretti et al. 2017). The mean redshift $z_{\rm cl}$ and the rest-frame velocity dispersion $\sigma_{\rm cl}$ of each cluster were derived using the biweight robust location and scale estimators (Beers et al. 1990) and applying an iterative 3σ clipping. Galaxies were considered cluster members if they lie within $3\sigma_{\rm cl}$ from the cluster redshift. R_{200} was computed from $\sigma_{\rm cl}$ following Poggianti et al. (2006) and used to scale the distances from the Brightest Cluster Galaxy (BCG).

The spectroscopic catalog has been corrected for both geometrical and magnitude incompleteness, using the ratio of the number of spectra yielding a redshift to the total number of galaxies in the parent photometric catalog, calculated both as a function of V magnitude and radial projected distance from the BCG.

Galaxy properties have been derived by fitting the fiber spectra with SINOPSIS (SImulatiNg OPtical Spectra wIth Stellar population models), a spectrophotometric model fully described in Fritz et al. (2007, 2011, 2014). It is based on a stellar population synthesis technique that reproduces the observed optical galaxy spectra. All the main spectrophotometric features are reproduced by summing the theoretical spectra of simple stellar populations of 12 different ages (from 3×10^6 to approximately 14×10^9 years).

The code provides estimates of star formation rates (SFRs), stellar masses (M_*), both observed and absolute model magnitudes, and measures of observed equivalent widths (EWs) for the most prominent spectral lines, both in absorption and in emission. Magnitudes were computed by convolving the filters response curves with the spectrum.

Due to the configuration of the 2dFdr spectrograph, which is a dual-beam system with two arms overlapping around 5700 Å, for each object observed with this instrument we obtained two spectra, hereafter called red and blue, that are spliced into the full final spectrum. Despite the quite extended overlap, the region of the spliced spectrum results is often quite noisy due to normalization issues.

While none of the lines used in our analysis (see Section 3) fall in the spliced region, the SFRs and mass estimates in such a region might be significantly affected by noise, therefore, we fit the continuum only on the blue part of the spectra, ranging from about 3600 Å–5700 Å.

Hereafter, we will use stellar masses locked into stars, including both those that are still in the nuclear-burning phase, and remnants such as white dwarfs, neutron stars, and stellar black holes.

We note SINOPSIS is fed with fiber spectra,[9] therefore all of the galaxy properties suffer from aperture effects. The fiber diameters were 2.″16 (AAT) and 1.″6 (WHT), therefore the spectra cover only the central 1.3–2.8 kpc of our galaxies depending on the cluster redshift, (see Cava et al. 2009 for details), which correspond to approximately half of the typical effective diameter of WINGS galaxies.[10] To recover the galaxy-wide integrated properties, all the derived quantities have been scaled from the fiber to the total magnitude, using the ratio of total to aperture fluxes.

For the WINGS sample, morphological types were derived from V-band images using MORPHOT, an automatic tool for galaxy morphology, purposely devised in the framework of the WINGS project (Fasano et al. 2012). MORPHOT extends the classical CAS classification using 20 different morphological diagnostics and assigns a morphological type (MORPHOT type, T_M) to each galaxy from -6 (cD) to 11 (irregulars). The morphological classification of the OmegaWINGS sample is currently underway (G. Fasano et al. 2017, in preparation). For our purposes, one of us (G.F.) visually classified the morphologies of the PSB galaxies in our sample (see Section 4) that were not in the original WINGS sample by inspecting the V-band images.

In the following, we will consider three main morphological classes: ellipticals ($-5 \leqslant T_M < -4.25$), S0s ($-4.25 \leqslant T_M \leqslant 0$), and late types ($T_M > 0$).

3. The Spectral Classification

The focus of this paper is the characterization of the properties of galaxies showing different features on their spectra, therefore we rely on the measure of the EWs provided by SINOPSIS. We convert the observed EWs in rest-frame values, simply dividing the measurements by $(1 + z)$; we adopted the usual convention of identifying emission lines with negative and positive ones.

Fritz et al. (2007) found that both absorption and emission lines are reliably measured by SINOPSIS in spectra with S/N > 3, calculated across the whole spectral range. In spectra

[9] Fibers are centered on the source emission profile with an accuracy that is equal or better than 0.″1 (see Gullieuszik et al. 2015).

[10] Effective radii were computed with GASPHOT by D'Onofrio et al. (2014); the median value of the circularized effective radius is $\sim$1.7 $\pm$ 0.2 kpc.

with S/N < 3, noise can be misinterpreted as an emission. This happens especially for the [O II] emission line, which is located in a spectral range where the hydrogen lines of the Balmer series (in absorption) crowd. It is hence possible that a peak between two such absorption lines is misinterpreted as an [O II] emission. In spectra with S/N $\leqslant 3$, the EW of the [O II] is $\geqslant -2$ Å, and we use this value as threshold above which measurements are considered unreliable. In our sample, the average S/N, calculated for the whole spectral range, is $\sim$12. Only 2% of the spectra have S/N < 3, therefore they are a negligible fraction.

Based on the spectral classification originally proposed by Dressler et al. (1999) and Poggianti et al. (1999) and more recently updated by Fritz et al. (2014), we subdivide our sample into three classes, according to the rest-frame EWs of [O II] and Hδ, which are good indicators of current and recent star formation. When the [O II] is not detected, the EW of [O III] and Hβ are also used. Differently from Fritz et al. (2014), our spectral classification also exploits the information on the Hα line: all spectra showing Hα in emission are directly classified as EML galaxies, regardless of the other lines. In this way we obtain a more robust classification, ensuring that there is no current star formation, in both the passive and PSB samples. The detailed description and the physical interpretation of this classification is discussed by Poggianti et al. (1999; 2009) and Fritz et al. (2014). Briefly, spectra with any of the aforementioned emission lines belong to galaxies in which the star formation is taking place, and will thereafter be called EML galaxies. Spectra with no emission lines, including Hα, are divided based on the strength of Hδ: k spectra, normally found in passively evolving elliptical galaxies, resembling those of K-type stars, with weak Hδ in absorption (H$\delta > 3$ Å), and k+a and a+k spectra, displaying a combination of signatures typical of both K- and A-type stars with strong Hδ in absorption (respectively, $3 <$ H$\delta < 8$ Å and H$\delta > 8$ Å). The former (k-type) will be thereafter called passive galaxies (PAS), the latter (both $k + a$ and $a + k$) PSB galaxies.

We note that, among the PSBs, the strength of Hδ is indicative of the initial condition associated with the main quenching event. Indeed a H$\delta > 6$ Å can be explained only if a burst of star formation involving high-mass fractions (10%–20%) happened prior to the sudden quenching. Galaxies showing this feature are caught in an early phase of transition (Goto 2004). In contrast, spectra with a moderate Hδ line could be both the result of the truncation of star formation in a normal star-forming galaxy (thus no burst is required) or a late stage of evolution of the proper PSB galaxies. Broadly speaking, while all PSB galaxies with strong Hδ will later turn into PSBs with moderate Hδ, the opposite is not true. Therefore, we will sometimes discuss also the strong PSB (H$\delta > 6$ Å, hereafter sPSB) separately.

The automatic classification has been visually confirmed. Upon inspection, we noticed that in a number of cases the code had misidentified emission lines (oxygen forbidden lines and Hβ), measuring noise rather than real emission. The [O II] emission lines, by coincidence, is located in a critical region of our spectra, being in the shortest wavelength regime covered by the spectrograph that often results to be quite noisy (see Smith et al. 2004). Moreover, we found that, in most cases, the Hβ and [O III] emissions were misidentified in spectra showing only one emission line.

Table 1
Cluster Sample: Global Properties

Cluster	z	$N_{\rm mem}$	$\sigma_{\rm cl}$ (km s^{-1})	R_{200} (Mpc)	log(L_X) (10^{44} erg s^{-1})
A1069	0.0651	130	695 ± 55	1.67	43.98
A151	0.0538	248	738 ± 32	1.78	44.0
A1631a	0.0465	369	760 ± 29	1.84	43.86
A168	0.0453	141	547 ± 38	1.32	44.04
A193	0.0484	101	764 ± 58	1.85	44.19
A2382	0.0639	322	698 ± 30	1.67	43.96
A2399	0.0577	291	730 ± 35	1.75	44.0
A2415	0.0578	194	690 ± 38	1.66	44.23
A2457	0.0587	249	680 ± 37	1.63	44.16
A2717	0.0498	135	544 ± 47	1.32	44.0
A2734	0.0618	220	781 ± 49	1.88	44.41
A3128	0.0603	480	839 ± 29	2.02	44.33
A3158	0.0594	357	1024 ± 37	2.46	44.73
A3266	0.0596	678	1319 ± 40	3.17	44.79
A3376	0.0463	263	845 ± 42	2.04	44.39
A3395	0.0507	369	1206 ± 55	2.91	44.45
A3528	0.0545	262	1017 ± 46	2.45	44.12
A3530	0.0549	275	674 ± 39	1.62	43.94
A3556	0.048	359	669 ± 35	1.62	43.97
A3558	0.0486	442	1003 ± 34	2.42	44.8
A3560	0.0491	283	840 ± 35	2.03	44.12
A3667	0.0558	386	1011 ± 42	2.43	44.94
A3716	0.0457	327	849 ± 27	2.05	44.0
A3809	0.0626	244	554 ± 38	1.33	44.35
A3880	0.058	216	688 ± 56	1.66	44.27
A4059	0.049	229	752 ± 38	1.82	44.49
A500	0.0682	227	791 ± 44	1.89	44.15
A754	0.0545	338	919 ± 37	2.22	44.9
A85	0.0559	172	982 ± 55	2.37	44.92
A957x	0.0451	92	640 ± 47	1.55	43.89
A970	0.0589	214	844 ± 49	2.03	44.18
IIZW108	0.0486	171	612 ± 38	1.48	44.34

Note. Columns: (1) cluster name, (2) cluster mean redshift, (3) number of member galaxies (used to compute mean redshift and velocity dispersion as explained in the text), (4) cluster velocity dispersion with errors, (5) R_{200} in Mpc, (6) logarithm of the X-ray luminosity (from Ebeling et al. (1996)).

We visually inspected all of the spectra where only one emission line was detected and, if necessary, changed the galaxy spectral type. Furthermore, we checked all of the k+a and a+k candidates and excluded those with undetected emission lines, remeasured the Hδ EW for those with an automatic measure higher than 5 Å or with a comparable uncertainty.

As already discussed in the previous section, we note that due to the limited size of the fiber diameter, we classify galaxies based on the spectra targeting only the central region of galaxies. The aperture bias could, in principle, lead to a misclassification of galaxies that may have remaining star formation activity outside the fiber.

4. Data Sample

One of the main focuses of this paper is the occurrence of PSB galaxies as a function of cluster-centric distance; in particular we want to investigate the role of the cluster environment also beyond the virial radius. We therefore restrict our analysis to the clusters covered also by OmegaWINGS observations. Among these, only the 32 clusters with a global

Table 2
Weighted Spectral Numbers and Fractions

Galaxy Type	PAS		PSB		sPSB		EML	
	N	(%)	*N*	(%)	*N*	(%)	*N*	(%)
Clusters	8162 (4235)	55.7 ± 0.4	1057 (560)	7.2 ± 0.2	154 (80)	1.1 ± 0.3	5441 (3029)	37.0 ± 0.4
Field	415 (225)	19.7 ± 0.8	28 (15)	1.3 ± 0.2	7 (3)	0.3 ± 0.1	1667 (923)	79.0 ± 0.9

Note. Weighted number (raw numbers in brackets) and percentage of the different spectral types for the magnitude-limited sample weighted for spectroscopic incompleteness and considering only galaxies inside $1.2R_{200}$. The field sample has no radial limits. The proportion of PAS (k), PSB ($k+a/a+k$), strong PSB (the subsample of PSB with EW(Hδ > =6), and EML galaxies are listed along with binomial errors.

spectroscopic completeness higher than ≈50% are used. The final cluster sample is presented in Table 1.

Galaxies belonging to the final sample have a V magnitude brighter than 20.

In our analysis, we neglect the contribution from active galactic nuclei (AGNs). As pointed out by Alatalo et al. (2016), this choice could bias our results in the sense that galaxies in which emission lines are not linked to the star formation process, but are excited by the AGN mechanism, are excluded from the PSB sample. Nonetheless, Guglielmo et al. (2015), analyzing a mass-limited sample extracted from the original WINGS survey, estimated that the AGN contribution in the star-forming galaxy population is approximately 1.6% and we estimate that this fraction will not remarkably change in our sample. Thus, including these objects in the EML galaxy population should not considerably affect our results. A more detailed analysis of EML galaxies and their classification as star-forming galaxies, transition objects, and AGNs for the WINGS sample is presented by Marziani et al. (2016).

The main sample consists of cluster members within $1.2R_{200}$ from the BCG, a distance that is reached by almost all the selected clusters (90%). We exclude galaxies at larger distances (the maximum radial coverage is approximately $2R_{200}$ for member galaxies) because these all belong to clusters with very low-velocity dispersion, so they might be a biased population not representative of the general one. We also exclude BCGs, which are a peculiar population (e.g., von der Linden et al. 2007; Fasano et al. 2010, and references therein).

Non-cluster member galaxies with $0.035 < z < 0.08$ constitute our field control sample, used for reference.

The final sample consists of 7824 cluster galaxies and 1163 field galaxies (respectively 14660 and 2110 galaxies, once weighted for incompleteness, see Cava et al. 2009 for a detailed explanation). The number of EML, PAS, and PSB galaxies in the different environments is given in Table 2 and discussed below.

5. Results

In this section, we present our results. We will first investigate the occurrence and the galaxy properties of the different spectral types (e.g., stellar masses, magnitudes, colors, and morphologies), then we will investigate trends as a function of both cluster-centric distance and the level of substructures in clusters. We will also focus on the position of the galaxies on the phase space and characterize the role of global cluster properties, i.e., cluster velocity dispersion and X-ray luminosity, in driving trends. The aim of our analysis is to shed light on the processes that induce a truncation of star formation on short timescales and give rise to the existence of the PSB galaxies. Given our interest in this population, in Figure 1 we show the composite spectrum of our PSBs to visualize the main features of this population. The composite spectrum is obtained by summing the spectra of all of the PSB galaxies in the cluster sample, after normalizing each spectrum by its mean value. The measured rest-frame EW(Hδ) is greater than 4 Å, the other Balmer lines are well visible and no emission is detected.

5.1. Properties of the Different Galaxy Populations

Table 2 presents the incidence of the different spectral types in clusters and in the field. PAS galaxies dominate the galaxy population in clusters, being 55.7 ± 0.4% of all galaxies, while EML galaxies are 37.0 ± 0.4% of all members. In the field, the contribution of the PAS and EML populations is reversed: nearly the 80% of field galaxies show signs of ongoing star formation, while less than 20% are PAS. The fraction of PSB galaxies is significantly higher in clusters than in the field: 7.2 ± 0.2% versus 1.3 ± 0.2%. We note that our field sample might actually be biased toward galaxies belonging to filaments or structures falling into the main cluster, but we are not able to separate them. Furthermore, there are only 15 PSBs in the field, therefore the statistics in this environment are too poor to draw any conclusion. A more complete analysis of PSB galaxies in the field in the local universe, based on a different sample, is currently underway (A. Paccagnella et al. 2017, in preparation).

The relevance of the PSB cluster population is even more striking considering their fraction relative to the active population, which includes galaxies that are (EML) or have been (PSB) star-forming within the last 2 Gyr. The PSB to active fraction gives the "quenching efficiency" (see Poggianti et al. 2009) that is the efficiency in truncating the star formation in star-forming galaxies. PSB galaxies represent 16.3 ± 0.5% of the cluster active population, in agreement also with the high-redshift fractions derived by Poggianti et al. (2009), while they make up less than 2% in the field. Hence, clusters are far more efficient than the field in shutting off star formation in galaxies on a very short timescale.

Stellar mass and absolute V magnitude (M_V) weighted distributions for galaxies of the different spectral types are presented in Figure 2. The spectral classification, going from PAS to PSB to EML galaxies, turns out to be, in both environments, a sequence of decreasing mean galaxy mass and increasing mean M_V. EML galaxies dominate the low-mass/low-luminosity tails of the distributions, while the contribution of the PAS population becomes more important going toward higher masses and luminosities. In order to test if the mass and magnitude distributions of the three populations are significantly different, we perform a Kolmogorov–Smirnov (K–S) test. The results, comparing the distributions of PSBs to PASs and EMLs and PASs to EMLs, allow us to reject the null

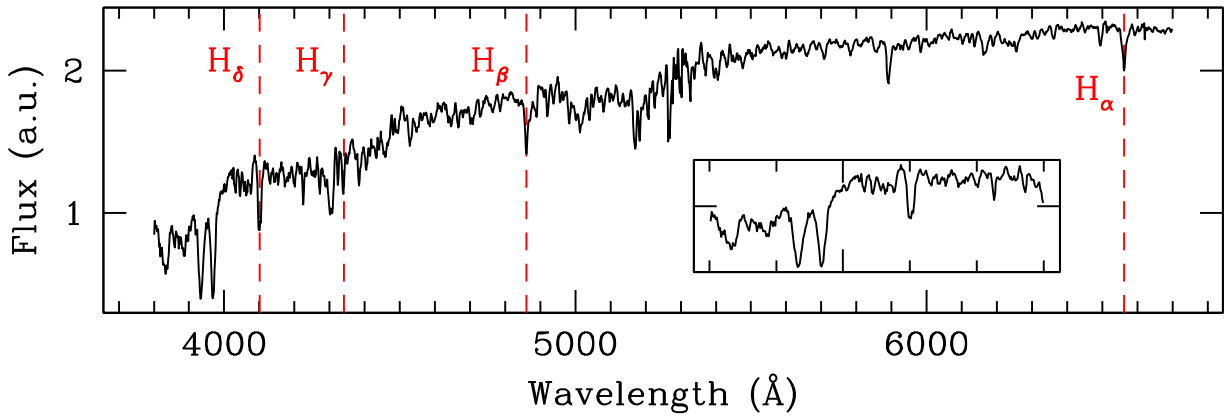

Figure 1. Rest-frame composite spectrum of the post-starburst cluster sample. The inset shows a zoom in of the spectral region around Hδ.

hypothesis that these populations are drawn from the same sample (P-values on the order of 0.0). This picture fits the downsizing scenario (Cowie et al. 1996), in which star formation at higher redshifts was more active in more massive/luminous galaxies that are the first to turn into passive.

The distributions of the properties of PSB galaxies are intermediate between those of the PAS and EML populations. This is even clearer looking at the median values of the distributions for cluster galaxies indicated by the black arrows in Figure 2 (the median masses are 9.78 ± 0.01, 9.98 ± 0.02, and 10.23 ± 0.1, the median magnitudes are -18.64 ± 0.02, -18.52 ± 0.04, and -19.09 ± 0.02 for EMLs, PSBs, and PASs, respectively).

Field median values agree, within the standard errors, with the cluster ones, apparently indicating no strong environmental dependencies. However, we remind the reader that the field sample size does not allows us to draw solid conclusions.

The absolute magnitude distribution of PSBs peaks around $M_V = -18.5$, with a deficit among the brightest galaxies ($M_V < -20.5$) with respect to both the EML and PAS populations. These characteristics were already visible in the sample described in Fritz et al. (2014) and are similar to those of the PSB population in the Coma cluster (Poggianti 2004). In the cluster sample, $14 \pm 1\%$ of the PSB galaxies are classified as sPSB; in the field, only 3/15 PSB galaxies are sPSB, making any conclusion statistically meaningless.

sPSB galaxies (dark green histograms in Figure 2) span a narrower range of both absolute magnitude ($M_V > -19$) and stellar mass ($\log M_* < 10.5$) missing the high-mass tail and luminosity. This suggests that only the least massive/luminous PSB galaxies undergo a phase of sPSB and confirms the hypothesis that while all of the sPSB galaxies will age and evolve into moderate PSB galaxies, not all PSBs have experienced the sPSB phase.

Figure 3 shows the absolute rest-frame color–magnitude diagram ($(B-V)$ versus M_V) for cluster galaxies of the different spectral classes.[11] To subdivide galaxies into red and blue, we consider the color–magnitude red sequence of each WINGS cluster given in Valentinuzzi et al. (2011). We use the average value of the slope across all clusters and fix the quote 1σ below the average red sequence. Galaxies whose color lie above

$$(B-V)_{\rm rf} = -0.045 \times V - 0.035$$

(black heavy line in Figure 3) are assigned to the red sequence, the rest to the blue cloud.

As expected, most PAS galaxies present red colors ($73.3 \pm 0.5\%$), while EML galaxies are preferably blue ($75.2 \pm 0.6\%$). Also, the majority of PSB and sPSB galaxies have red colors ($73 \pm 1\%$ and $59 \pm 4\%$, respectively), even though the fraction of PSBs with blue colors is not negligible. This finding supports the idea that the fast quenching of star formation immediately brings the galaxies to the red sequence, but also that a pure color-based selection is unable to uniquely distinguish between passive star-forming and galaxies that recently interrupted their star formation. Therefore, a detailed spectral analysis is necessary to recognize the different galaxy subpopulations.

According to the picture we described above, one would expect sPSB galaxies to have bluer colors than the rest of the PSBs (see, e.g., Poggianti 2004). Figure 3 shows that this seems not to be the case in our sample. This result might be due to the fact that, at low redshift, most of the stars in galaxies are old, and, as soon as the star formation is switched off, the galaxy becomes quickly red as the old stars dominate the integrated light. An alternative explanation could be the presence of dust. As already discussed in Poggianti et al. (1999), the assumption that the progenitors of PSB galaxies are dusty starburst objects entails that dust reddening might affect also the PSB class. We tested this hypothesis by exploiting the average extinction values given by SINOPSIS and no trend with the EW of Hδ was found. This result might suggests that either sPSB galaxies are not more obscured than PSBs, or that the real EW values in absence of dust obscuration should be higher and that our EW estimates have to be considered as lower limits.

5.2. Morphologies

The analysis of the morphologies of PSBs can shed light on the typical properties of this population. Table 3 presents the percentage of galaxies of different morphological types for the whole PSB sample. $45 \pm 2\%$ of the galaxies are classified as S0s, while the remaining sample is evenly divided between ellipticals ($28 \pm 1\%$) and late types ($27 \pm 1\%$).

Considering only sPSB galaxies, while the fraction of S0s does not change within the errors ($41 \pm 4\%$), that of late types and elliptical do: the former represent $42 \pm 4\%$ of the total population, the latter $17 \pm 3\%$.

[11] We recall that absolute magnitudes and rest-frame colors were computed on the fiber spectrum and are given by the spectrophotometric model convolving the filters response curves with the spectrum.

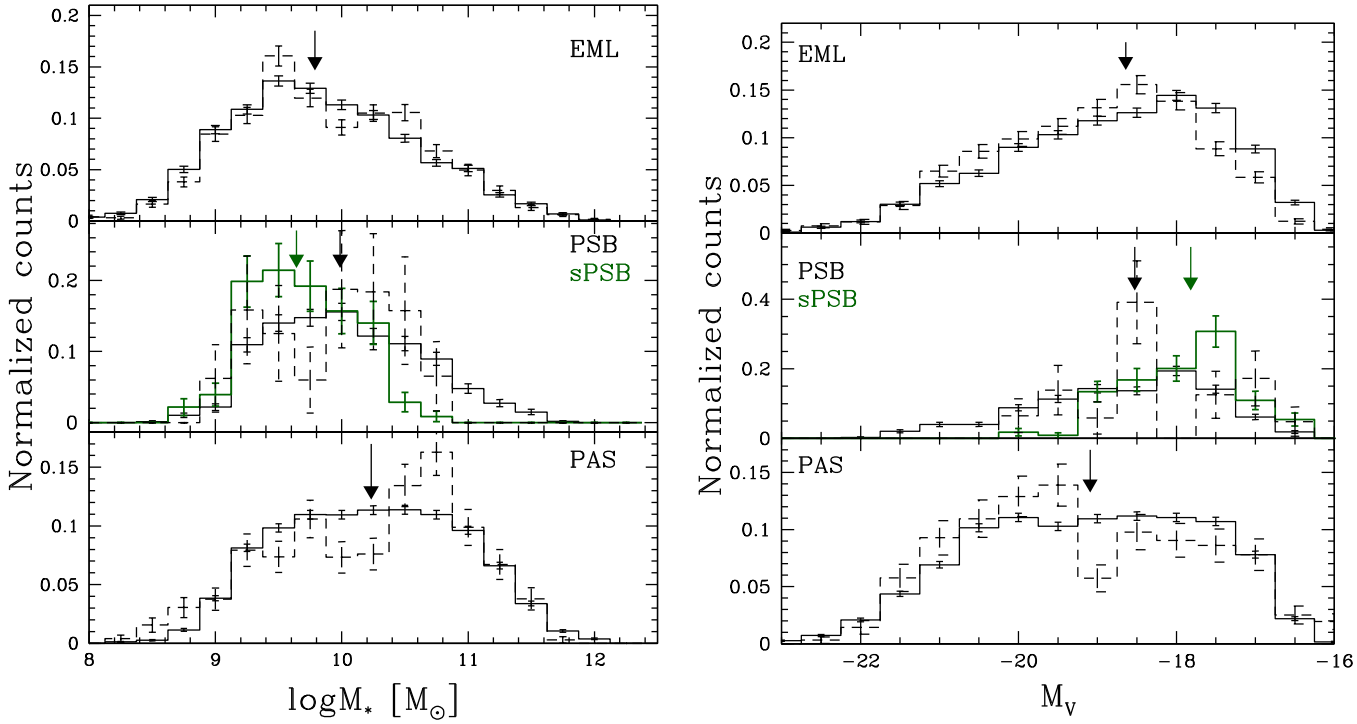

Figure 2. Number of cluster (solid) and field (dashed) galaxies in the three main spectral types as a function of stellar mass (left panel) and absolute V magnitude (right panel). Dark green histograms in the middle panels show the sPSB subsample. Arrows indicate the median value for each type. Errors are Poissonian (Gehrels 1986).

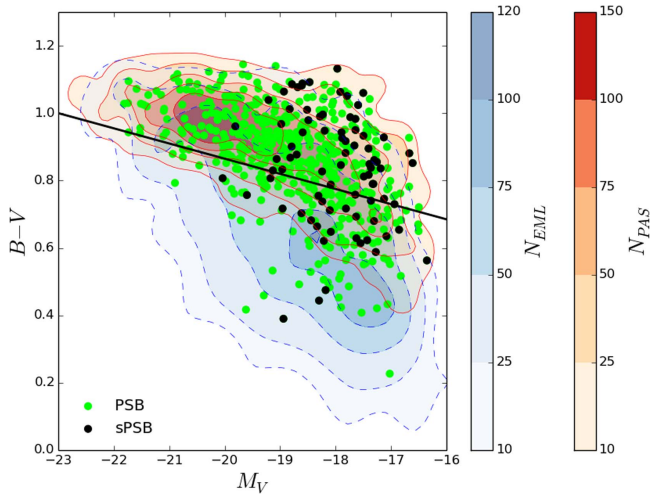

Figure 3. Rest-frame $(B-V)$–V relation for cluster galaxies of the different spectral types. Red-solid and blue-dashed contours are the number densities of PAS and EML galaxies, respectively. Green dots: PSB; black dots: sPSB. The black line represents the selection limit we adopt to select red and blue galaxies.

Table 3
Weighted Morphological Percentages of PSB Galaxies

	E (%)	S0 (%)	LT (%)
PSB	28 ± 1	45 ± 2	27 ± 1
sPSB	17 ± 3	41 ± 4	42 ± 4

Note. Morphological percentages for the PSB and sPSB samples weighted for spectroscopic incompleteness. Errors are binomial.

Several reasons might be at the origin of such different morphological distributions between the two samples. The larger fraction of late types among sPSB galaxies than among PSBs agrees with the hypothesis that these are younger objects in which the original disk structure has not yet been changed. Together with mass and luminosity distribution of sPSB galaxies (Figure 2), this morphological mix could also indicate that the process responsible for the strong burst needed to create the observed spectral features is more effective on less massive galaxies with a high fraction of gas at the moment of infalling. As an alternative, invoking only ram-pressure stripping as the main process responsible for the production of both PSB and sPSB galaxies, the observed morphologies could simply reflect the properties of the infalling population. We remind the reader that at low redshifts, the amount of gas necessary to produce a burst of star formation as a consequence of the interaction of the galaxy with the ICM, via ram-pressure stripping, is mostly located in low-mass late-type systems, while more massive galaxies are mostly early types and gas deficient (Mahajan 2013).

Similarly to the analysis of galaxy colors, the analysis of the morphologies shows that the majority of PSB galaxies cannot be recognized when using just a morphological classification, but a detailed spectral analysis is necessary.

5.3. Spatial Distribution of the Different Spectral Types

In the previous sections, we have shown that low-z clusters host a much larger fraction of PSB galaxies than the field, pointing toward a cluster-specific origin of the majority of this class of objects. To differentiate among possible quenching processes that can suddenly truncate star formation in clusters, we now investigate the radial distribution of the different spectral classes. Overall, the cluster-centric distance is a good tracer of the cluster density profile, is related to the time since

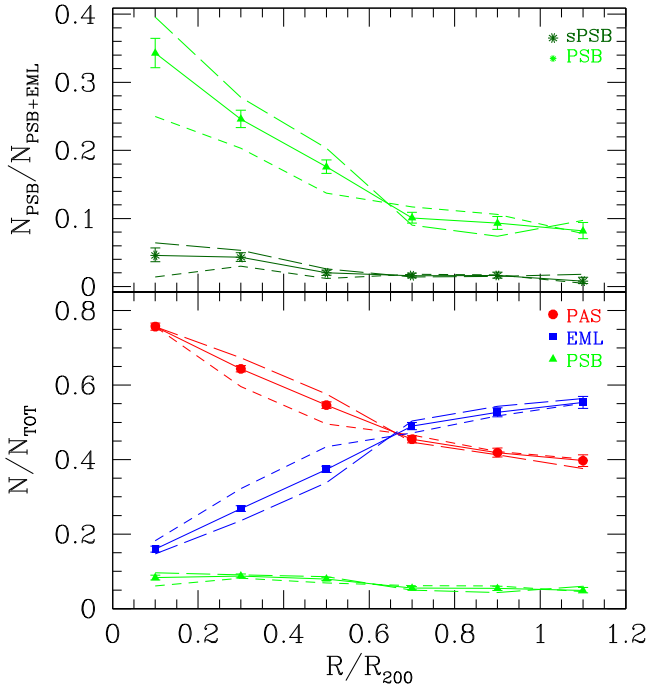

Figure 4. Ratio of post-starburst to active galaxies (top panels) and ratio of post-starburst, passive, and emission-line galaxies to the total (bottom panels) as a function of R/R_{200}. Points with error bars represent cluster fractions, dashed lines give the trends of the respective fractions in two bins of velocity dispersion σ ($\sigma < 840$ km s^{-1}—short dashed lines—and $\sigma > 840$ km s^{-1}—long dashed lines). Errors are binomial (Gehrels 1986).

infall into the cluster (Goto 2004), and is an approximate timescale sensitive to processes occurring on times on the order of a few Gyr. Processes that quench star formation gradually, such as strangulation, would induce radial gradients, while processes acting on short timescales, e.g., ram-pressure stripping, are more likely to cause distinctive signatures at the radii where they are most effective.

The bottom panel of Figure 4 shows the incidence of each galaxy population (PAS, EML, PSB) as a function of cluster-centric projected distance, in units of R/R_{200}.

As mentioned in Section 4, we limit our analysis to $1.2R_{200}$, not to bias our results toward the clusters with low values of velocity dispersion. In agreement with previous results, (Weinmann et al. 2006; von der Linden et al. 2010; Vulcani et al. 2015) we find a pronounced relation between distance from the cluster center and the composition of the galaxy population. PAS galaxies dominate the inner regions ($\sim$70% at $R < 0.4R_{200}$), and their fraction decreases going outward of a factor of $\sim$2.5. In contrast, the fraction of EML galaxies is $\sim$60% at large cluster-centric distances and rapidly declines toward the cluster center of a factor of four. Despite their relatively small incidence, the fraction of PSB galaxies also depends on cluster-centric distance, and their trend follows that of PAS: in the cluster cores, PSBs are $\sim$1.7, as numerous as PSBs in the outskirts.

The upper panel of Figure 4 shows the quenching efficiency (PSB/(PSB + EML)) as a function of the cluster-centric distance. In the cluster cores, the ratio is $\sim$35%, indicating that even in these regions EMLs dominate the active population. The fraction decreases of a factor of three from the cluster center to $0.6R_{200}$, while it is almost constant in the outer regions ($R/R_{200} > 0.7$). Also, the incidence of sPSBs (dark green symbols in the upper panel of Figure 4) among the active population increases toward the center, even if with a less steep trend. These results might arise due to the different proportions in the population mix as a function of the global environment, i.e., different cluster halo mass. We therefore consider in Figure 4 two different cluster velocity-dispersion bins, respectively higher (long dashed line) and lower (short dashed line) than[12] 840 km s^{-1}, and find that the trends persist and are even more pronounced in the high-cluster-mass bin. A more detailed analysis of the dependence of the PSB fraction on the cluster global properties will be discussed in Section 5.6.

Considering the PSBs of different morphological types, we find that overall the incidence of ellipticals, S0s, and late types does not change with cluster-centric distance, suggesting there is no morphological segregation for PSBs (plot not shown).

5.4. Substructures

Clusters are generally characterized by the presence of substructures (Biviano et al. 2002; Ramella et al. 2007), which implies that merging between clusters and groups is a rather common physical process of cluster formation. This merging process has been found to affect greatly star formation histories of member galaxies and to eventually induce secondary starburst (see Bekki 1999, 2010; Cohen et al. 2014). The coincidence of the position of the strongest $k+a$ galaxies and the X-ray substructures in Coma found by Poggianti (2004) strengthens this scenario.

To check whether the presence of substructures alters the star formation in cluster galaxies, we compute the fractions of the PSB galaxies belonging to these systems. We use the catalogs of the WINGS substructures presented by A. Biviano et al. (2017, in preparation), who define substructures and assign member galaxies to potential substructures exploiting the velocity distributions of galaxies in the cluster local density peaks.

30.4 ± 0.4% of the member galaxies belong to substructures and, among these, 6.1 ± 0.4% are PSB galaxies and 0.9 ± 0.2% are sPSBs. The percentage of the PSBs is slightly lower than the value found for the same population when considering the entire galaxy sample (7.2 ± 0.2%). The same conclusion holds for the fraction of PSB and sPSB galaxies with respect to the active population. Thus, this type of analysis does not reveal a strong PSB enhancement in substructures.

We also investigate the fraction of PSB, PAS, and EML galaxies in clusters characterized by different levels of relaxation. We use the parameter SUB defined in Biviano et al. (2017, in preparation) that depends, among other things, on the fraction of member galaxies belonging to substructures, and consider three types of clusters: relaxed (SUB = 0), partly relaxed (SUB = 1), and unrelaxed (SUB > 1). In agreement with, e.g., Cohen et al. (2015) and Biviano et al. (1997), we find a higher/lower fraction of EML/PAS galaxies in less relaxed clusters than in more relaxed ones (0.344 ± 0.005/0.580 ± 0.005, 0.408 ± 0.0084/0.522 ± 0.009, and 0.44 ± 0.01/0.50 ± 0.01 for SUB = 0, SUB = 1, and SUB > 1, respectively). Even more interestingly, the fraction of PSB galaxies also depends on the dynamical state of the cluster, following the trend of the PAS population: the PSB/PSB +EML fractions are 0.179 ± 0.006, 0.144 ± 0.009, and 0.12 ± 0.01 for SUB = 0, 1, and >1, respectively. This is

[12] The value 840 km s^{-1} was chosen to approximately divide the galaxy sample in two equally populated bins.

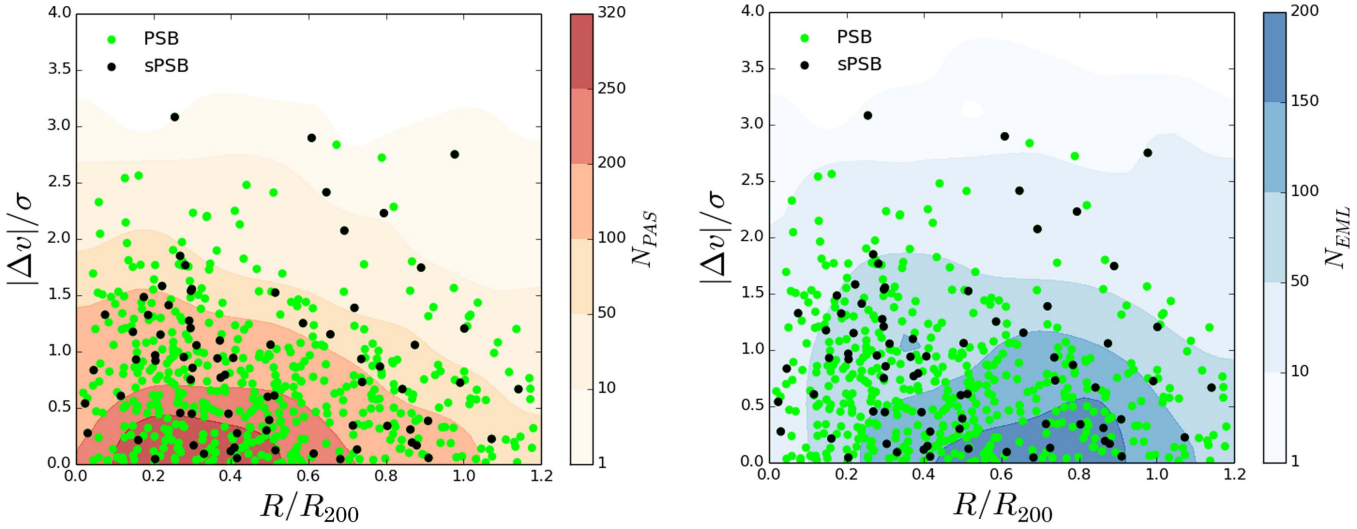

Figure 5. Observed stacked phase-space diagram for cluster members. Cluster-centric distances are in units of R_{200} and the absolute value of the line-of-sight velocities with respect to the cluster recessional velocities are normalized by the velocity dispersion of the cluster. PSB galaxies are represented by green points, sPSB galaxies by black points. They are over-plotted to PAS galaxies (left panel, red contours) and to EML galaxies (right panel, blue contours).

the opposite of what might be expected if merging clusters were the most favorable environment for PSB production. Part of this trend might be due to the existence of the correlation between PSB fraction and L_X (Figure 7), as the average X-ray luminosity decreases going from more-relaxed to less relaxed clusters (2.8, 2.7 and 1.3×10^{44} erg s^{-1} for SUB $= 0$, 1, >1). Moreover, the most unrelaxed clusters are in a sense clusters still in the formation process in which the galaxy populations are still very similar to the unprocessed population of galaxies in the merging groups/clusters, therefore they are still very rich in star-forming galaxies that have not yet experienced a massive cluster environment.

5.5. Phase-space Analysis

Many recent papers (Biviano et al. 2002; Haines et al. 2013; Oman et al. 2013; Muzzin et al. 2014; Jaffé et al. 2016) have shown that galaxy populations with different dynamical histories are well separated in the so-called phase space, which links the spatial position of a galaxy in the clusters, in units of R_{200}, and its peculiar velocity, Δv, normalized by the velocity dispersion of the cluster σ. Moreover, the theoretical phase-space diagram derived from cosmological simulations retains information of the epoch of accretion of a galaxy, that can therefore be estimated based on the location of the galaxy in the diagram (Haines et al. 2015). The same is unfortunately not possible with observations, given the large uncertainties that induce the different populations to overlap on the plane. However, it is still possible to retrieve important clues about the dynamical histories of the different galaxy populations in clusters (e.g., Mahajan et al. 2011; Oman et al. 2013; Hernández-Fernández et al. 2014; Muzzin et al. 2014; Haines et al. 2015; Jaffé et al. 2015, 2016). Indeed, the overall distribution of galaxies in the phase space strongly depends on the infall times: galaxies that were accreted earlier (i.e., virialized galaxies) typically occupy a triangular-shaped region while that were recently accreted or with infalling population permeate all projected velocities and radii. Combining this evidence with the well-established correlation between galaxy quiescence and environment, PAS galaxies are expected to form the majority of the virialized population while EML and PSB galaxies should belong to the infall or recently accreted sample.

Figure 5 shows the projected phase space obtained by combining all clusters together for the different subpopulations separately. As expected, PAS galaxies are typically found in a triangular-shaped virialized region, which corresponds to the low-velocity–low-distance area, while EML galaxies are more spread in both radius and velocity. The PSB population, as already discussed, preferentially lie at small cluster-centric distances ($R > 0.6R_{200}$), exhibiting a non-negligible spread in velocity. A 2D K–S test rejects the hypothesis that both PSB and EML and, with a slightly less significance, PSB and PAS galaxies are drawn from the same distribution (P-values, respectively, of 0.0 and 0.07), suggesting indeed that these populations are in different stages of their virialization process. The sPSB population can be better distinguished in terms of velocity rather than cluster-centric distance: following the general radial trend of PSB galaxies, these galaxies have slightly higher velocities (median $\Delta v/\sigma$ of 0.67 ± 0.02 and 0.87 ± 0.07 for the PSB and sPSB populations, respectively).

To better quantify the differences between the populations, modeling the results presented by Haines et al. (2015) for 75 simulated clusters at $z = 0.0$, Figure 6 shows the mean normalized line-of-sight (LOS) velocity dispersion of each subpopulation ($\sigma_{\rm LOS}/\sigma$) in six bins of projected radial distance. The errors are obtained using the classical jackknife technique (Efron 1982). Due to the low number statistics, the sPSB sample is divided only in three bins spanning the same radial range.

By comparison with the analysis of Haines et al. (2015), the different velocity-dispersion profiles can be explained according to the dynamical evolution and accretion history of the galaxy populations. PAS and EML galaxies are well separated, the former having low LOS-velocity dispersion at all radii with respect to the latter that displays, especially in the cluster core, higher values of σ. These trends are best reproduced by the virialized population, which was accreted at early epochs ($z > 0.4$), and by the most recently accreted and backsplash populations, respectively (Gill et al. 2005) The profile of the PSB population follows the one traced by the PAS/virialized

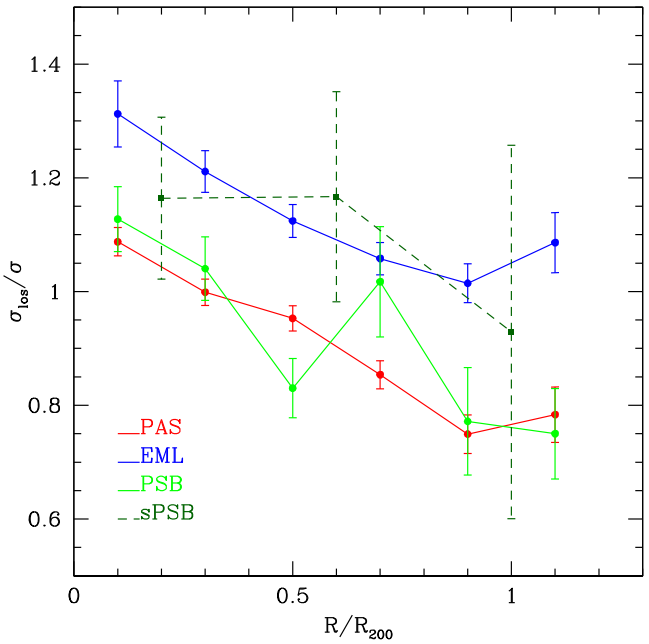

Figure 6. Velocity-dispersion profiles ($\sigma_{\rm LOS}(r)/\sigma$) of each galaxy population; colors refer to the different populations as described in the labels and as in Figure 4. Errors are jackknife standard deviations (Efron 1982).

population, while sPSBs have remarkably larger velocity dispersions thus belonging to the more recently accreted population.

These findings well fit the scenario in which the strength of the EW(Hδ) sets a timeline with higher values indicating a more recent quenching event. If the sPSBs are the consequence of a starburst prior to a sudden quenching, the violent/sudden event that triggers the burst seems to happen on first infall; moderate PSBs could originate in the same way but are observed longer time after quenching (Poggianti et al. 2009).

This result moves in the same direction of Muzzin et al. (2014) who, investigating the location of different classes of galaxies on the stacked phase space of clusters at $z \sim 1$, found that PSB galaxies are commonly found at small cluster-centric radii with high cluster-centric velocities.

5.6. Dependence of the Spectral Type Fractions on Cluster Properties

So far we have shown how the fractions of the different subpopulations change as a function of the spatial location, both physical and dynamical, within the clusters.

We now examine if and how the fraction of PSB galaxies depends on the global properties of the clusters, such as velocity dispersion and X-ray luminosity, both proxy for the system total mass. It is still unclear whether or not the cluster mass affects the amount of observed star formation. For example, several studies at high and intermediate redshifts (e.g., Finn et al. 2005; Poggianti et al. 2006) find an inverse correlation between star formation and cluster mass, while others (e.g., Popesso et al. 2007) assert that no such correlation exists in the nearby cluster population.

All of our clusters contain galaxies belonging to all the three main spectral classes, but the population mix in each cluster is quite different. To assess if these differences arise from a dependence on the cluster halo mass, for each cluster we compute the PSB fraction, weighted for completeness, among all galaxies and among the active population. For this analysis, we restricted the data to an absolute magnitude-limited sample. This should prevent the introduction of possible systematics related to the selection criteria of the cluster sample. Member galaxies brighter than $M_V = -17.4$ were selected. This is the absolute magnitude corresponding to the $V = 20$ apparent magnitude limit of the most distant cluster.

The results are shown in Figure 7 where the individual systems, indicated as black points, are shown as a function of velocity dispersion (left) and X-ray luminosity (right).

To mark the average trends we group the cluster sample into five bins of σ and L_X with approximately the same number of galaxies and show the results as red points. Both fractions (PSB/all and PSB/active galaxies) increase with the mass of the system, more significantly when we consider the X-ray luminosity rather than the velocity dispersion. A Spearman test, which assesses how well the relationship between two variables can be described using a monotonic function performed on the unbinned data, yields a 99.8% (99.9%) and 98.1% (99.3%) probability of a correlation of the PSB/all (PSB/active) fraction with L_X and σ, respectively.

This result is in line with the findings of Poggianti et al. (2009) for clusters in the EDisCS sample at $z \sim 0.5$ even if the strength of the correlations for our sample is lower (the Spearman test yields a 99.1% and 99.7% probability of a correlation with the velocity dispersion of their PSB/all and PSB/active fractions, respectively). In contrast, it is at odds with the analysis performed by Fritz et al. (2014) on the restricted WINGS sample. These authors did not detect correlations with either the velocity dispersion or the X-ray luminosity. Discrepancies could be due to several reasons, such as the different selection criteria for PSB galaxies (they did not use the information on the H_α line), the different cut in magnitude, the higher completeness, or the larger area covered by our sample.

6. Discussion

By exploiting the capabilities of the combined WINGS and OmegaWINGS samples, in this paper we investigated the properties and the spatial distribution of galaxies that are currently star forming, that have recently interrupted their star formation, and that are already passive in clusters at $0.04 < z < 0.07$. Our main focus has been on PSB galaxies, to shed light on the processes that induce galaxies to undergo this particular phase during their life.

PSB galaxies are characterized by intermediate physical properties with respect to the EML and PAS galaxies, and are thought to be in a transition phase between these two populations: both their median stellar mass and magnitudes are in between the values found for the other two populations. As expected given the fact that they have no ongoing star formation, PSB galaxies present colors similar to the PAS galaxies, even though at faint magnitudes they can also be as blue as the EML galaxies.

Almost half of the PSBs galaxies have been classified as S0s, while the incidence of elliptical and late-type galaxies depends on the strength of the measured EW of Hδ: considering all PSBs, the fraction of ellipticals and late types is similar, considering only the sPSB, late-type galaxies dominate the population.

The fraction of PSB galaxies decreases with increasing distance, suggesting that in the core of the clusters some

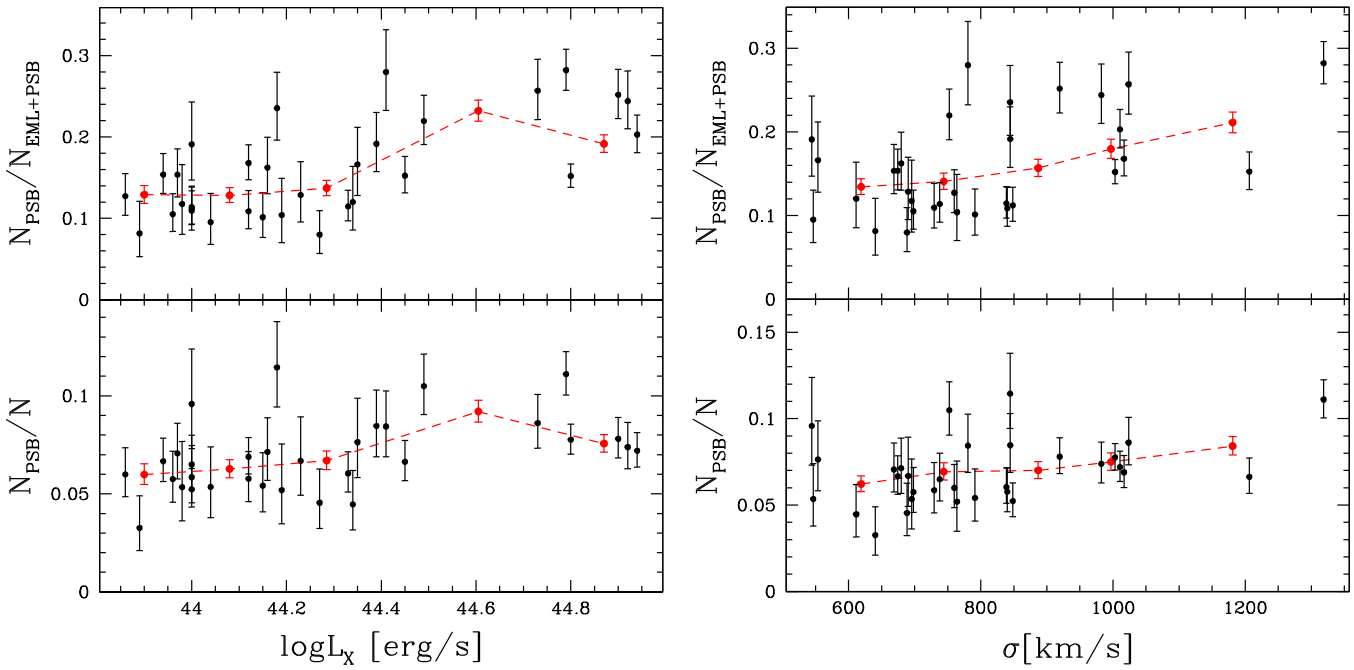

Figure 7. Fraction of post-starburst galaxies as a function of the cluster X-ray luminosity (left) and velocity dispersion (right). Black points represent individual clusters, red points give the fractions in five equally populated bins. Lower panels: weighted fraction of post-starburst galaxies among the whole population. Upper panels: weighted fraction of post-starburst galaxies among the active population. Errors are binomial.

mechanisms are inducing galaxy transitions. The same fraction also depends on the cluster properties and it steadily increases with increasing L_x and σ. Moreover, PSBs do not concentrate as much in the low cluster-centric distance–low-velocity locus of the phase space as virialized galaxies do. This, together with the fact that their velocity dispersion is quite intermediate between that of PAS and EML galaxies, especially for the sPSB galaxies, could lead to the interpretation that PSBs are a combination of galaxies with a mix of times since infall (backsplash + virialized). Ideally, one should define the virial, infall, and backsplash classes following the orbits of the particles using cosmological simulation. This task is beyond the scope of this work but will be addressed in forthcoming papers.

6.1. Slow and Fast Quenching Mechanisms in Clusters

As found by Poggianti (2004), Tran et al. (2007), and Muzzin et al. (2014), PSB galaxies have to be generated by a fast acting mechanism, given that this phase can last approximately 1–1.5 Gyr. As already discussed in Section 1, spectra showing strong Balmer absorption lines and no emission are the result of a precise combination of an old stellar population above which A-type star signatures are well visible. These stars, formed within the last Gyr, dominate the light of a galaxy where a recent star formation activity has ended abruptly and are visible for 1–1.5 Gyr (e.g., Poggianti 2004, and references therein). Even though this is a quite efficient channel to transform galaxies from star-forming to passive, it is definitely not the only one; e.g., Patel et al. (2009), Vulcani et al. (2010), and Paccagnella et al. (2016) found a population of galaxies in transition on long timescales (few Gyr) both in the local universe and at higher redshift ($z < 1$). Adopting a different approach, following the infall and orbits of galaxies in the vicinity of the 75 most massive clusters in the millennium cosmological simulation, Haines et al. (2015) also support a slow quenching scenario, with a timescale on the order of 0.7–2 Gyr.

Seeking for objects in transition from being star-forming to becoming passive, Paccagnella et al. (2016) analyzed the SFR–M_* relation of local cluster galaxies in a mass-limited sample extracted from the WINGS+OmegaWINGS sample. They identified a population of galaxies, called *transition galaxies*, located 1.5σ below the field SFR–M_* relation, whose star formation histories and properties suggest that they have had a reduced SFR for the past 2–5 Gyr. At least above the mass completeness limit, the fraction of transition galaxies strongly depends on environment, being almost negligible outside the virial radius and rising toward the center, making up for almost the 30% of star-forming galaxies inside $0.6R_{200}$. As concluded by the authors, these findings, together with the estimated quenching timescale, are consistent with the hypothesis that the interaction of galaxies with the intracluster medium via strangulation causes a gradual shut down of star formation.

We are now in the position of directly comparing the slow quenching channel characterized by Paccagnella et al. (2016) with the much faster one required to observe the typical PSB signatures. To do so, we consider only galaxies with stellar masses larger than the mass completeness limit of $10^{9.8}$ $M_\odot$ used by Paccagnella et al. (2016). 346 PSB galaxies (650 once weighted for completeness) enter the sample, of which only 32 (56) are sPSB. Above this limit, PSBs constitute $7.3 \pm 0.3\%$ of the total population and all of the environmental dependencies found for the whole sample persist. For comparison, above the same limit and the same cluster-centric distance, 408 (780) galaxies were classified by Paccagnella et al. (2016) as in transition, and they constitute $9.0 \pm 0.3\%$ of the entire population. By definition, being transition galaxies selected from the star-forming population, there is no object entering both samples.

Therefore transition galaxies are only slightly more numerous than PSB galaxies. Starting from the logical assumption

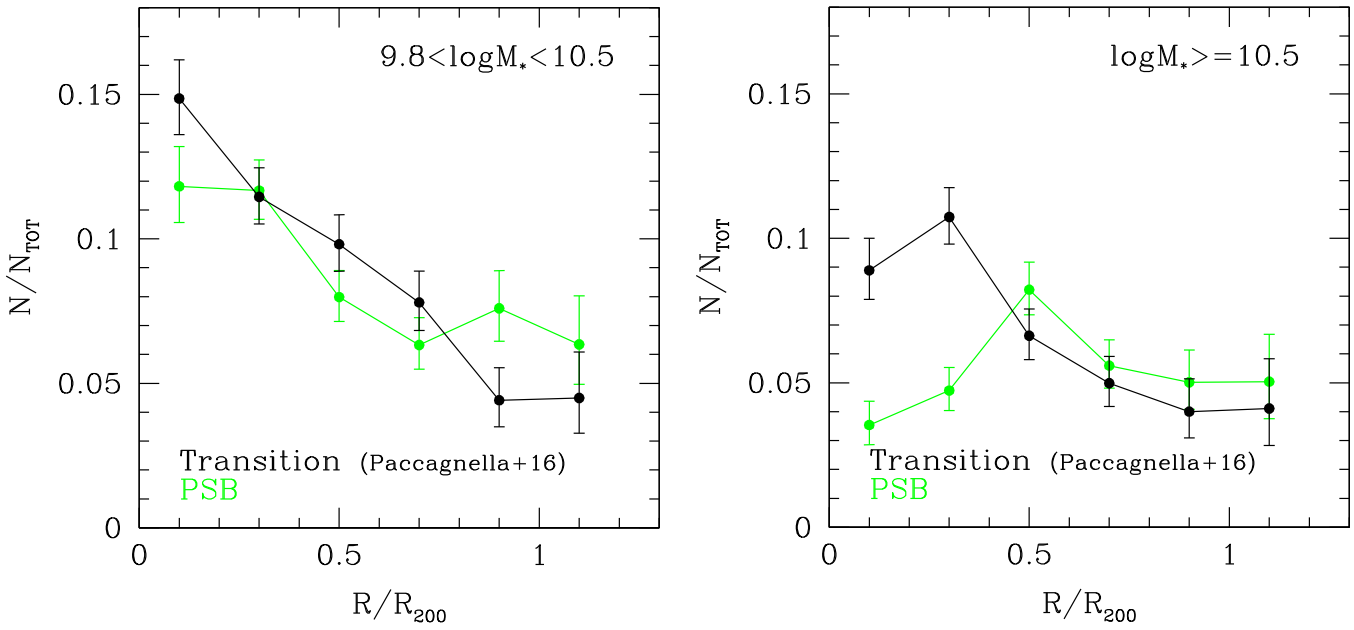

Figure 8. Radial distribution of transition galaxies (black) as defined by Paccagnella et al. (2016) and of PSB galaxies (green), in two bins of stellar mass. Errors are binomial.

that both populations have a common progenitor among star-forming galaxies, and if we assume that the transition phase lasts for about twice the time (on the order of >2 Gyr) of the PSB visibility (∼1 Gyr), we conclude that the short-timescale star formation "quenching" channel contributes at least two times more than the long timescale one to the growth of the passive population.

Figure 8 investigates in detail where these two populations are found within the clusters. It shows the number of transition and PSB galaxies to the total number of galaxies, as a function of cluster-centric distance. As done by Paccagnella et al. (2016), two different mass bins are considered here, to also look for trends with stellar mass. For $\log M_* < 10.5$, PSB and transition galaxies present a similar anticorrelation between the fraction of PSB and transition objects and distance, even though PSB galaxies show a slightly flatter trend, being less numerous than transition galaxies in the core of the clusters and slightly more numerous outside the virial radius.

For $\log M_* > 10.5$, at large cluster-centric distances, both populations present trends similar to those at lower masses, but in the cluster cores they present a drop in number. Such a drop occurs only in the cluster cores for transition galaxies, at $r < 0.5R_{200}$ for PSBs. Overall, it might be primarily due to the fact that in the cluster cores massive galaxies are already mostly passive, therefore the reservoir for transitioning galaxies is poorer than at lower masses. In addition, the different behavior seen for the two populations could be due to the visibility timescales of the two populations, with PSBs disappearing faster than transition galaxies on the way to the cluster core.

As mentioned in Section 2, galaxies drawn from the WINGS sample (approximately all those located within $0.6R_{200}$) have been morphologically classified. We can therefore compare the morphologies of PSB and transition galaxies in the core of the clusters, to look for signs of a link between galaxy morphology and timescale of quenching. We consider the mass-limited samples. Overall, among PSB galaxies, 40 ± 2% are ellipticals, 44 ± 2% are S0s, and the remaining 16 ± 2% are late-type galaxies. Transition galaxies have a much more numerous population of S0s, with a remarkable 56 ± 2% at the expense of elliptical galaxies, accounting only for the 28 ± 2%, while 16 ± 2% are late types.

No strong trends of the morphological mix with distance have been detected. However, we stress that here we are considering only galaxies in the core of the clusters and we are not attempting to extrapolate trends at larger distances, where the morphological mix might be different. In addition, we remind the reader that this analysis is performed above the mass completeness limit of $10^{9.8}\,M_\odot$ and that this cut excludes the vast majority of sPSB galaxies from our sample. This population has been found to have a distinct morphology from the whole population of PSB galaxies (see Section 5.1).

Studies regarding slow and fast quenching should necessarily follow different approaches. As far as the PSB population is concerned, due to the high precision clock imposed by A-type stars lifetimes, there is a general agreement on the timescales involved (see Poggianti 2004; Quintero et al. 2004; Poggianti et al. 2009; Muzzin et al. 2014; Vulcani et al. 2015, etc.) and, from these, different mechanisms have been proposed. On the other hand, a hypothesis on the physical processes causing the slow quenching of a galaxy has to be made to estimate the timescales involved. Several authors have tried to estimate the quenching timescales of satellite galaxies through different approaches. Wetzel et al. (2013) proposed a mass-dependent "delay-then-rapid" scenario in which star formation is quenched rapidly but only after a delay of 2–4 Gyr after infall. As an alternative Taranu et al. (2013) presented models where quenching occurs within a smaller radius, approximately $0.5R_{200}$, followed by an exponential decline of star formation over 3–3.5 Gyr.

6.2. Specific Processes Responsible for the Objects in Transitions in Clusters

We found the majority of transition and PSB galaxies within the virial radius. It seems clear from our results that any of the proposed physical mechanisms (i.e., starvation or ram-pressure

stripping) that alter the star formation of infalling galaxies is stronger in the central regions of the cluster, where the density and the temperature of the ICM (as well as the velocity of galaxies) reach their maxima. By comparing the cluster crossing times and the A-stars lifetime, we could also imagine an evolutionary sequence in which some of the PSBs (the low-mass ones, as discussed in Section 5.1) descend from sPSB galaxies, i.e., the ram pressure starts being effective at larger distances, generating the population of sPSB, while at smaller cluster-centric distances we only see the PSB galaxies. However, the comparison of the radial trend of the fractions of PSBs and transition galaxies does not allow to definitely ascertain whether the two populations have a different origin. Indeed, considering, for example, that ram-pressure stripping depends, among other things, on the orbit and on the orientation of the galaxy with respect to the ICM (Abadi et al. 1999), we can depict two different scenarios in which star formation can either be suddenly shut down (on timescales on the order of $\sim$1 Gyr, Muzzin et al. 2014) or gently and progressively depressed by ram-pressure stripping, and therefore give origin to the two observed galaxy populations.

In the first scenario, the resulting quenched population is expected to have PSB features, maintaining the original structural properties, since nothing apart from gas loss would disturb its morphology. Recall that the quenching timescale of PSB galaxies is imposed by A-type stars lifetime. In the second scenario, ram-pressure stripping might be the main responsible also for the transition population presented in Paccagnella et al. (2016). Nonetheless, the same population could originate also via strangulation, consistent with a gradual quenching corresponding to an exponential timescale of a 2 Gyr or more. Indeed, strangulation is expected to have the effect of removing the outer galaxy gas halo and prevent further infall of gas into the disk. On timescales of few Gyr, the star formation would thus exhaust the available gas, quenching the star formation activity.

In addition to ram-pressure stripping and strangulation, other mechanisms might play a role, even though they most likely take place at larger distances form the cluster center.

As discussed for example by Treu et al. (2003) and reviewed by Boselli & Gavazzi (2006), quenching from gravitational interaction between galaxies (i.e., galaxy–galaxy interactions, harassment) occurs preferentially outside the virial radius, given the high velocity dispersions in the cluster cores that remarkably reduce the probability of pair interactions, with timescales of the order of some 10^{10} year. Moreover, these interactions act on the stellar component, producing selective morphological transformations that we do not observe in the transition or PSB populations.

We emphasize that this does not mean that galaxy–galaxy interactions have no effect at all on cluster galaxies. These processes might eventually become important, but generally after the gas has been removed by other processes.

7. Summary and Conclusions

In this work, we have resorted to an observed magnitude-limited sample of galaxies in clusters drawn from the WINGS (Fasano et al. 2006; Moretti et al. 2014) and OmegaWINGS surveys (Gullieuszik et al. 2015; Moretti et al. 2017) to investigate the occurrence and the properties of galaxies of different types in 32 clusters at $0.04 < z < 0.07$. We classified the galaxies according to the different features detected in their spectra (presence/absence of O II, O III, Hδ, and Hα) into passive (PAS), PSB, and EML galaxies. We have compared stellar population properties and location within the clusters of the different spectral types to obtain valuable insights on the physical processes responsible for the star formation quenching.

The main results can be summarized as follows.

1. For $V < 20$, PAS represent $55.7 \pm 0.4\%$ of the cluster population within 1.2 virial radii, EML represent $37.0 \pm 0.4\%$, and PSBs $7.3 \pm 0.2\%$, 15% of which show strong Hδ in absorption (>6, sPSB), indication of either a very recent quenching and/or of a strong burst before quenching.
2. PSBs have stellar masses, magnitudes, colors, and morphologies intermediate between PAS and EML galaxies, typical of a population in transition from being star-forming to passive. Interestingly, 45% of PSBs have S0 morphology, $28 \pm 1\%$ are ellipticals, and $27 \pm 1\%$ are late types. Considering only sPSBs, the incidence of late types increases to $42 \pm 4\%$ with a corresponding drops of ellipticals, which are only $17 \pm 3\%$.
3. The incidence of PSBs slightly increases from the cluster outskirts toward the cluster center and from the least toward the most luminous and massive clusters, defined in terms of L_X and velocity dispersion.
4. The dynamical state of the clusters partially influences the incidence of PSBs. While the presence of substructures does not enhance the fraction of PSBs, the level of relaxation does: the fraction of PSBs is higher in relaxed clusters. At least part of this trend is due to the correlation between PSB fraction and L_X.
5. The phase-space analysis and the velocity-dispersion profiles suggest that PSBs represent a combination of galaxies with different accretion histories. Moreover, the PSBs with the strongest Hδ are consistent with being recently accreted.

PSBs are thought to be galaxies generated by fast acting mechanisms and this phase is expected to last approximately 1–1.5 Gyr (e.g., Poggianti 2004; Muzzin et al. 2014). Our analysis suggests that as a galaxy is accreted onto a cluster, at first its properties are not strongly affected, but when it approaches the virialized region of the cluster processes like ram-pressure stripping or other interactions induce either a burst of the star formation with a subsequent fast quenching, or simply a fast quenching. As the shut off of the star formation occurs, the galaxy changes the features in its spectrum, but variations in color and morphology require longer timescales, therefore PSBs appear with a wide range of these properties. It is important to stress that the majority of those galaxies that are truncated on a short timescale cannot be recognized based on color or color+morphology, but only by performing a detailed spectral analysis.

The fraction of PSBs is similar to the fraction of galaxies in transition on longer timescales, as defined by Paccagnella et al. (2016), suggesting that the short-timescale star formation quenching channel, lasting less than half the timescale required to slowly quench star formation, contributes two times more than the long timescale one to the growth of the passive population, therefore processes like ram-pressure stripping and interactions are more efficient than strangulation in affecting star formation, at least in clusters.

In other environments, the fraction of PSB galaxies and the processes responsible for its existence might be considerably

different. Vulcani et al. (2015) found hints of an enhanced fraction of PSB galaxies in groups compared to isolated and binary systems, but a complete characterization of the physical processes is still missing. In a forthcoming paper (A. Paccagnella et al. 2017, in preparation), we will characterize the incidence of PSB galaxies in the different environments, contrasting the properties of galaxies in clusters, groups, binary systems, and isolated galaxies to build a complete picture of the assembly of this population.

We thank the anonymous referee for their useful comments that helped us to improve the manuscript. A.P. acknowledges financial support from the Fondazione Ing. Aldo Gini and thanks the Anglo Australian Observatory for a productive stay during which part of this work was carried out. We acknowledge financial support from PRIN-INAF 2014 grant. B.V. acknowledges the support from an Australian Research Council Discovery Early Career Researcher Award (PD0028506). This work was co-funded under the Marie Curie Actions of the European Commission (FP7-COFUND).

References

Abadi, M. G., Moore, B., & Bower, R. G. 1999, MNRAS, 308, 947
Abraham, R. G., Smecker-Hane, T. A., Hutchings, J. B., et al. 1996, ApJ, 471, 694
Alatalo, K., Cales, S. L., Rich, J. A., et al. 2016, ApJS, 224, 38
Baldry, I. K., Glazebrook, K., Brinkmann, J., et al. 2004, ApJ, 600, 681
Balogh, M. L., Baldry, I. K., Nichol, R., et al. 2004, ApJL, 615, L101
Balogh, M. L., Navarro, J. F., & Morris, S. L. 2000, ApJ, 540, 113
Beers, T. C., Flynn, K., & Gebhardt, K. 1990, AJ, 100, 32
Bekki, K. 1999, ApJL, 510, L15
Bekki, K., Owers, M. S., & Couch, W. J. 2010, ApJL, 718, L27
Bekki, K., Shioya, Y., & Couch, W. J. 2001, ApJL, 547, L17
Biviano, A., Katgert, P., Mazure, A., et al. 1997, A&A, 321, 84
Biviano, A., Katgert, P., Thomas, T., & Adami, C. 2002, A&A, 387, 8
Blake, C., Pracy, M. B., Couch, W. J., et al. 2004, MNRAS, 355, 713
Blanton, M. R., Hogg, D. W., Bahcall, N. A., et al. 2003, ApJ, 594, 186
Boselli, A., & Gavazzi, G. 2006, PASP, 118, 517
Brinchmann, J., Charlot, S., White, S. D. M., et al. 2004, MNRAS, 351, 1151
Butcher, H. R., & Oemler, A., Jr. 1984, Natur, 310, 31
Caldwell, N., & Rose, J. A. 1997, AJ, 113, 492
Cava, A., Bettoni, D., Poggianti, B. M., et al. 2009, A&A, 495, 707
Cohen, S. A., Hickox, R. C., & Wegner, G. A. 2015, ApJ, 806, 85
Cohen, S. A., Hickox, R. C., Wegner, G. A., Einasto, M., & Vennik, J. 2014, ApJ, 783, 136
Cooper, M. C., Newman, J. A., Weiner, B. J., et al. 2008, MNRAS, 383, 1058
Couch, W. J., & Sharples, R. M. 1987, MNRAS, 229, 423
Cowie, L. L., Songaila, A., Hu, E. M., & Cohen, J. G. 1996, AJ, 112, 839
D'Onofrio, M., Bindoni, D., Fasano, G., et al. 2014, A&A, 572, A87
Dressler, A. 1980, ApJ, 236, 351
Dressler, A., & Gunn, J. E. 1982, ApJ, 263, 533
Dressler, A., & Gunn, J. E. 1992, ApJS, 78, 1
Dressler, A., Oemler, A., Jr., Couch, W. J., et al. 1997, ApJ, 490, 577
Dressler, A., Oemler, A., Jr., Poggianti, B. M., et al. 2013, ApJ, 770, 62
Dressler, A., Smail, I., Poggianti, B. M., et al. 1999, ApJS, 122, 51
Ebeling, H., Edge, A. C., Allen, S. W., et al. 2000, MNRAS, 318, 333
Ebeling, H., Edge, A. C., Bohringer, H., et al. 1998, MNRAS, 301, 881
Ebeling, H., Voges, W., Bohringer, H., et al. 1996, MNRAS, 281, 799
Efron, B. 1982, The Jackknife, the Bootstrap and other Resampling Plans (Philadelphia, PA: SIAM)
Fasano, G., Bettoni, D., Ascaso, B., et al. 2010, MNRAS, 404, 1490
Fasano, G., Marmo, C., Varela, J., et al. 2006, A&A, 445, 805
Fasano, G., Poggianti, B. M., Bettoni, D., et al. 2015, MNRAS, 449, 3927
Fasano, G., Vanzella, E., Dressler, A., et al. 2012, MNRAS, 420, 926
Finn, R. A., Zaritsky, D., McCarthy, D. W., Jr., et al. 2005, ApJ, 630, 206
Fritz, J., Poggianti, B. M., Bettoni, D., et al. 2007, A&A, 470, 137
Fritz, J., Poggianti, B. M., Cava, A., et al. 2011, A&A, 526, A45
Fritz, J., Poggianti, B. M., Cava, A., et al. 2014, A&A, 566, A32
Gehrels, N. 1986, ApJ, 303, 336
Gill, S. P. D., Knebe, A., & Gibson, B. K. 2005, MNRAS, 356, 1327
Goto, T. 2004, A&A, 427, 125
Goto, T. 2005, MNRAS, 357, 937
Goto, T., Nichol, R. C., Okamura, S., et al. 2003, PASJ, 55, 771
Guglielmo, V., Poggianti, B. M., Moretti, A., et al. 2015, MNRAS, 450, 2749
Gullieuszik, M., Poggianti, B., Fasano, G., et al. 2015, A&A, 581, A41
Gunn, J. E., & Gott, J. R., III 1972, ApJ, 176, 1
Haines, C. P., Pereira, M. J., Smith, G. P., et al. 2013, ApJ, 775, 126
Haines, C. P., Pereira, M. J., Smith, G. P., et al. 2015, ApJ, 806, 101
Hernández-Fernández, J. D., Haines, C. P., Diaferio, A., et al. 2014, MNRAS, 438, 2186
Hogg, D. W., Masjedi, M., Berlind, A. A., et al. 2006, ApJ, 650, 763
Jaffé, Y. L., Smith, R., Candlish, G. N., et al. 2015, MNRAS, 448, 1715
Jaffé, Y. L., Verheijen, M. A. W., Haines, C. P., et al. 2016, MNRAS, 461, 1202
Kauffmann, G., Heckman, T. M., White, S. D. M., et al. 2003, MNRAS, 341, 54
Kauffmann, G., White, S. D. M., Heckman, T. M., et al. 2004, MNRAS, 353, 713
Larson, R. B., Tinsley, B. M., & Caldwell, C. N. 1980, ApJ, 237, 692
Lewis, I., Balogh, M., De Propris, R., et al. 2002, MNRAS, 334, 673
Mahajan, S. 2013, MNRAS, 431, L117
Mahajan, S., Mamon, G. A., & Raychaudhury, S. 2011, MNRAS, 416, 2882
Marziani, P., D'Onofrio, M., Bettoni, D., et al. 2016, arXiv:1608.07924
Mihos, J. C., & Hernquist, L. 1994, ApJL, 425, L13
Mok, A., Balogh, M. L., McGee, S. L., et al. 2013, MNRAS, 431, 1090
Moore, B., Katz, N., Lake, G., Dressler, A., & Oemler, A. 1996, Natur, 379, 613
Moran, S. M., Ellis, R. S., Treu, T., et al. 2007, ApJ, 671, 1503
Moretti, A., Gullieuszik, M., Poggianti, B., et al. 2017, arXiv:1701.02590
Moretti, A., Poggianti, B. M., Fasano, G., et al. 2014, A&A, 564, A138
Muzzin, A., van der Burg, R. F. J., McGee, S. L., et al. 2014, ApJ, 796, 65
Newberry, M. V., Boroson, T. A., & Kirshner, R. P. 1990, ApJ, 350, 585
Oman, K. A., Hudson, M. J., & Behroozi, P. S. 2013, MNRAS, 431, 2307
Omizzolo, A., Fasano, G., Reverte Paya, D., et al. 2014, A&A, 561, A111
Paccagnella, A., Vulcani, B., Poggianti, B. M., et al. 2016, ApJL, 816, L25
Patel, S. G., Holden, B. P., Kelson, D. D., Illingworth, G. D., & Franx, M. 2009, ApJL, 705, L67
Pimbblet, K. A., Smail, I., Kodama, T., et al. 2002, MNRAS, 331, 333
Poggianti, B. M. 2004, in Clusters of Galaxies: Probes of Cosmological Structure and Galaxy Evolution, ed. J. S. Mulchaey, A. Dressler, & A. Oemler (Cambridge: Cambridge Univ. Press), 245
Poggianti, B. M., Aragón-Salamanca, A., Zaritsky, D., et al. 2009, ApJ, 693, 112
Poggianti, B. M., & Barbaro, G. 1996, A&A, 314, 379
Poggianti, B. M., & Barbaro, G. 1997, A&A, 325, 1025
Poggianti, B. M., Smail, I., Dressler, A., et al. 1999, ApJ, 518, 576
Poggianti, B. M., von der Linden, A., De Lucia, G., et al. 2006, ApJ, 642, 188
Popesso, P., Biviano, A., Romaniello, M., & Böhringer, H. 2007, A&A, 461, 411
Quintero, A. D., Hogg, D. W., Blanton, M. R., et al. 2004, ApJ, 602, 190
Ramella, M., Biviano, A., Pisani, A., et al. 2007, A&A, 470, 39
Salpeter, E. E. 1955, ApJ, 121, 161
Schawinski, K., Urry, C. M., Simmons, B. D., et al. 2014, MNRAS, 440, 889
Smith, G. A., Saunders, W., Bridges, T., et al. 2004, Proc. SPIE, 5492, 410
Taranu, D. S., Dubinski, J., & Yee, H. K. C. 2013, ApJ, 778, 61
Tran, K.-V. H., Franx, M., Illingworth, G., Kelson, D. D., & van Dokkum, P. 2003, ApJ, 599, 865
Tran, K.-V. H., Franx, M., Illingworth, G. D., et al. 2007, ApJ, 661, 750
Tran, K.-V. H., Franx, M., Illingworth, G. D., Kelson, D. D., & van Dokkum, P. 2004, in IAU Coll. 195, Outskirts of Galaxy Clusters: Intense Life in the Suburbs, ed. A. Diaferio, 483
Treu, T., Ellis, R. S., Kneib, J.-P., et al. 2003, ApJ, 591, 53
Valentinuzzi, T., Poggianti, B. M., Fasano, G., et al. 2011, A&A, 536, A34
Valentinuzzi, T., Woods, D., Fasano, G., et al. 2009, A&A, 501, 851
Varela, J., D'Onofrio, M., Marmo, C., et al. 2009, A&A, 497, 667
von der Linden, A., Best, P. N., Kauffmann, G., & White, S. D. M. 2007, MNRAS, 379, 867
von der Linden, A., Wild, V., Kauffmann, G., White, S. D. M., & Weinmann, S. 2010, MNRAS, 404, 1231
Vulcani, B., Poggianti, B. M., Finn, R. A., et al. 2010, ApJL, 710, L1
Vulcani, B., Poggianti, B. M., Fritz, J., et al. 2015, ApJ, 798, 52
Weinmann, S. M., van den Bosch, F. C., Yang, X., & Mo, H. J. 2006, MNRAS, 366, 2
Wetzel, A. R., Tinker, J. L., Conroy, C., & van den Bosch, F. C. 2013, MNRAS, 432, 336
Wheeler, C., Phillips, J. I., Cooper, M. C., Boylan-Kolchin, M., & Bullock, J. S. 2014, MNRAS, 442, 1396